

****Volume Title****

*ASP Conference Series, Vol. **Volume Number***

****Author****

© ****Copyright Year**** *Astronomical Society of the Pacific*

MHD simulations of a supernova-driven ISM and the warm ionized medium using a positivity preserving ideal MHD scheme

Mordecai-Mark Mac Low^{1,4,9}, Alex S. Hill^{2,3}, M. Ryan Joung⁴,
Knut Waagan⁵, Christian Klingenberg⁶, Kenneth Wood⁷,
Robert A. Benjamin⁸, Christoph Federrath^{9,10,11}, and L. Matthew Haffner²

¹*Dept. of Astrophysics, American Museum of Natural History, 79th St. at Central Park W., NY, NY, 10024, USA*

²*Dept. of Astronomy, U. Wisconsin-Madison, Madison, WI, USA*

³*CSIRO Astronomy & Space Science, Marsfield, NSW, Australia*

⁴*Dept. of Astronomy, Columbia U., NY, NY, USA*

⁵*CSCAMM, U. Maryland at College Park, College Park, MD, USA*

⁶*Dept. of Mathematics, U. Würzburg, Würzburg, Germany*

⁷*School of Physics & Astronomy, St. Andrews U., St. Andrews, Scotland, UK*

⁸*Dept. of Physics, U. Wisconsin-Whitewater, Whitewater, WI, USA*

⁹*ZAH, Inst. für Theoretische Astrophysik, U. Heidelberg, Heidelberg, Germany*

¹⁰*CRAL, ENS Lyon, Lyon, France*

¹¹*Monash Centre for Astrophysics, School of Mathematical Sciences, Monash U., Victoria, Australia*

Abstract. We present new 3D magnetohydrodynamic (MHD) simulations of a supernova-driven, stratified interstellar medium. These simulations were run using the Waagan et al. (2011) positivity preserving scheme for ideal MHD implemented in the Flash code. The scheme is stable even for the Mach numbers approaching 100 found in this problem. We have previously shown that the density distribution arising from hydrodynamical versions of these simulations creates low-density pathways through which Lyman continuum photons can travel to heights $|z| > 1$ kpc. This naturally produces the warm ionized medium through photoionization due primarily to O stars near the plane. However, our earlier models reproduce the peak but not the width of the observed emission measure distribution. Here, we examine whether inclusion of magnetic fields and a greater vertical extent to the simulation domain produce a gas distribution that better matches the observations. We further study the change of magnetic energy over time in our models, showing that it appears to reach a steady state after a few hundred megayears, presumably supported by a turbulent dynamo driven by the supernova explosions.

1. Observational Motivation

Supernova explosions provide one of the major sources of energy for observed turbulent motions in the interstellar gas. It can be argued that in star forming regions of galaxies their influence predominates (Mac Low & Klessen 2004; Tamburro et al. 2009). To constrain their influence on the interstellar gas, we have compared observations of the upper atmosphere and gaseous halo of the Galaxy to numerical simulations of supernova-driven turbulence.

The base model that we used, described by Joung & Mac Low (2006) and Joung et al. (2009), and inspired by the work of Avillez (2000), used version 2.4 of the Flash code (Fryxell et al. 2000) to model a square section through a stratified galactic disk centered on the midplane, with dimensions $0.5 \times 0.5 \times 10$ kpc and periodic boundary conditions in the horizontal direction. The vertical boundary conditions were taken to be constant pressure to allow outflow. The adaptive mesh refinement capability of Flash was used to fix the maximum resolution within 200 pc of the midplane to 1.95 pc, with reduced maximum resolution at higher altitudes for computation efficiency. Supernova explosions were placed at both random and correlated locations to reproduce their distribution in the Galaxy. Radiative cooling was implemented with an equilibrium ionization, solely temperature dependent cooling function, and a diffuse heating term characteristic of photoelectric heating and stratified with altitude was also included.

Henley et al. (2010) measured X-ray emission from the hot, gaseous halo of the Galaxy by using shadowing against relatively nearby clouds to remove contributions from local sources including solar wind charge exchange and emission from the Local Bubble. They then compared these observations to simulations of emission from our models. They found good agreement between the simulated and observed emission measure of hot gas looking out of the Galaxy. However, the effective temperature of the emission in the model systematically climbed with time.

Wood et al. (2010) compared the distribution of $H\alpha$ emission measures measured by the Wisconsin $H\alpha$ Mapper (WHAM Haffner et al. 2003) along lines of sight out of the plane of the Galaxy to the distribution of simulated $H\alpha$ emission from the model (see Fig. 1(a)). Figure 1(b) shows the comparison. They found that the emission measure distribution of the models was centered around the same value as the observations, but that it was broader, with more lines of sight having very high or low emission measures seen in the models. This suggested that some additional homogenizing effect might be acting beyond the physics included in the models. Magnetic fields could have such an effect, so we decided to investigate how their inclusion would change our results. We here report on our implementation of fields in our models and some first results, though we only reach preliminary conclusions.

2. Simulation Techniques

Our problem requires the computation of flows with Alfvén and Mach numbers greatly exceeding unity in plasmas with a range of plasma β (ratio of thermal to magnetic pressure) extending from well under to well over unity. Most linearized Riemann solvers have substantial stability problems under these conditions. Therefore we used the positivity-preserving generalization by Bouchut et al. (2007) of an HLL (Harten et al. 1983) approximate Riemann solver with a base MUSCL-Hancock scheme. This solver satisfies discrete entropy inequalities and imposes positivity of density and in-

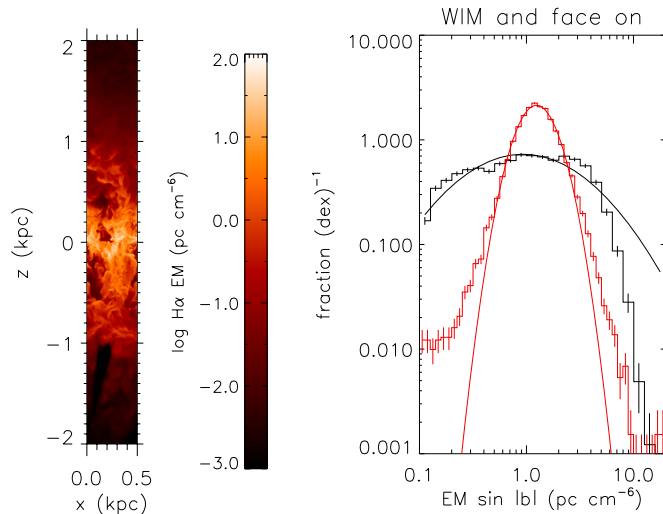


Figure 1. (a) Edge-on visualizations of emission measures ($\int n_e^2 ds$) from a simulation grid described by Joung et al. (2009). Adapted from Fig. 3 of Wood et al. (2010). (b) Emission measure distributions for the Galactic DIG from the WHAM survey and from our photoionization simulation. Fraction (dex) $^{-1}$ is the fraction of points in each bin divided by the logarithmic bin interval. The black histogram is of $\int n_e^2 ds$ in the simulation, viewed face-on. The red histogram is of $EM \sin |b|$ from the WHAM survey with classical H II regions and sightlines with $|b| < 10^\circ$ removed, from Hill et al. (2008). Lognormal fits to each distribution are also shown. For the emission measures from the simulations we have removed contributions from midplane regions with $|z| < 150$ pc. Adapted from Fig. 6 of Wood et al. (2010).

ternal energy. The three-wave HLL3R version of Bouchut et al. (2010) is used here, in an implementation described by Waagan (2009). This solver vastly improves stability, and thus efficiency, without sacrificing accuracy.

Waagan et al. (2011) demonstrates that HLL3R performs as well as other HLL schemes on standard test problems such as shock tubes. Figure 2 shows a comparison of solutions of an Orszag-Tang vortex by two of the standard Flash solvers, Roe and HLL3R to the HLL3R solution. The accuracy compares to the Roe solver, while the slightly more diffusive HLL3R solver fails to capture the central structure. However, the comparison of the performance of the Roe solver to HLL3R for driven Mach 2 turbulence given in Table 3 of Waagan et al. (2011) shows that the Roe solver requires a Courant-Friedrich-Lewy number below 0.2 for stability, while HLL3R remains stable at 0.8. Even when the Roe solver doesn't crash outright, it regularly generates hot zones that force the Courant timestep to low values. As a result, the total CPU time used for this problem is a factor of 9 lower for HLL3R. Increasing the Mach number to 10 in $\beta = 1$ plasma resulted in a problem that simply could not be stably computed by the Roe or HLL3R solvers, but was solved by HLL3R. This stability was demonstrated under even more extreme conditions in the driven MHD turbulence models by Brunt et al. (2010) which reached Mach numbers as high as 20 with $\beta = 1.25 \times 10^{-3}$.

Our magnetized, supernova-driven models were initialized with constant β fields having midplane strengths of either 6.5 or 13 μ G. We found during initial testing that the grid we used in Joung & Mac Low (2006) and Joung et al. (2009) was insufficiently

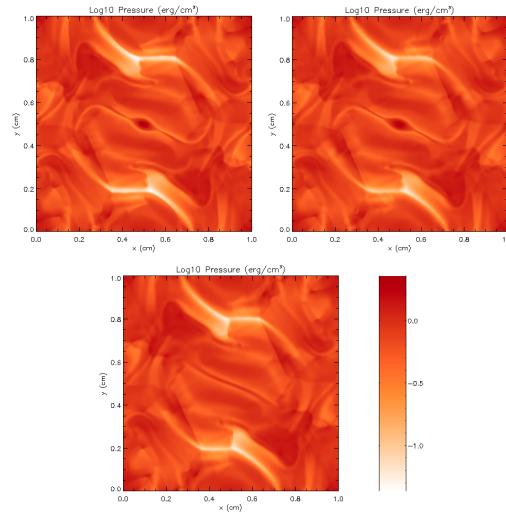


Figure 2. Orszag-Tang test. Pressure at time $t = 1$ with resolution $h = 256^1$. Top to bottom, left to right: FLASH-Roe, HLL3R, FLASH-HLLE. Figure 4.3 from Waagan et al. (2011)

large to capture the dynamics of the halo, though it sufficed to model the midplane gas that we focused on in those papers. Instead, we used $1 \times 1 \times 40$ kpc grids for our standard models. Also, instead of initializing an entirely isothermal grid at 10^4 K, we set the halo temperature to 10^6 K at altitudes $|z| > 1$ kpc to avoid very strong shocks at high altitude during the initial expansion of supernova blast waves.

3. Preliminary Results

3.1. Vertical Structure

The magnetic field indeed leads to somewhat smoother flows, with more filamentary structure seen above a kiloparsec. However, the biggest surprise came from examination of the vertical structure of the halo. The ever increasing halo temperature seen by Henley et al. (2010) was shown to be a numerical artifact. The constant-pressure vertical boundary conditions used by Joung & Mac Low (2006) and Joung et al. (2009) did not have a velocity limiter to prevent inflow. After a hot initial transient flow from the first supernova explosions in the halo crossed the boundary, the pressure and temperature were set high. The gas then started to fall inward lacking further support, and the boundary then fed high pressure and temperature continuously on to the grid. Raising the boundary and setting it to allow only outflow resulted in much more reasonable behavior, with an appropriately thick disk not confined by high pressure gas, and a moderate temperature halo, as shown in Figure 3. In future work we will examine in detail whether the effective X-ray temperature, $H\alpha$ emission measure, and $H\text{ I } 21\text{ cm}$ distributions now reproduce the observations.

However, we then saw that even in steady state, the halo undergoes vertical oscillation on either side of the midplane, uncorrelated between the upper and lower sides. Exactly this behavior was predicted by Walters & Cox (2001) using a one-dimensional

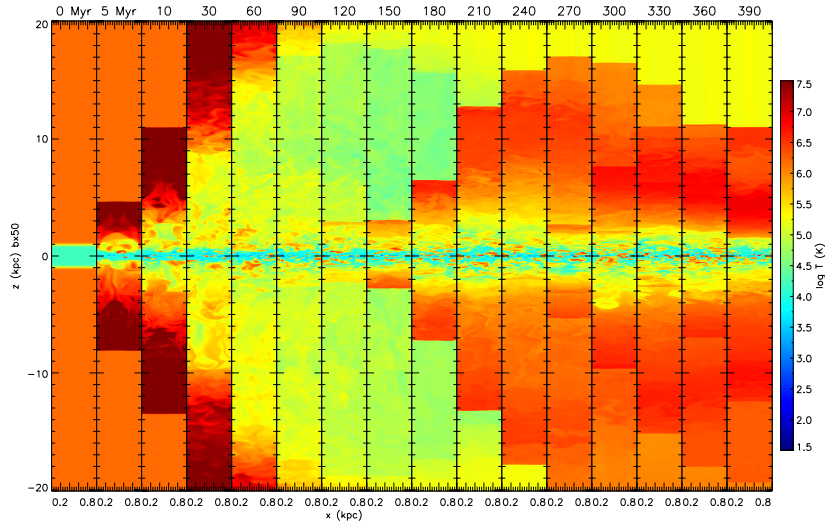


Figure 3. Slices of temperature over time for a model with initial midplane magnetic field of $6.5 \mu\text{G}$. The time of each slice in megayears is listed above each image. Note that the aspect ratio is not unity; the vertical scale of these images is contracted. Adapted from Figure 2 of Hill et al. (2011)

model and proposed as an explanation for the remarkable observation that gas towards the northern Galactic pole seems to be primarily infalling while that towards the southern Galactic pole seems to be primarily flow outwards. Although our models reproduce only a small portion of a galactic disk, we may take from them the qualitative statement that the upper atmospheres and halos of galaxies are unlikely to be quiescent, static places, but rather are likely to be in continuous hypersonic motion, with observable consequences.

3.2. Dynamios

The modeling of an idealized turbulent dynamo using HLL3R was already demonstrated by Waagan et al. (2011). This work was extended to consider dynamios in accretion flows with application to the formation of the first stars by Sur et al. (2010). Federrath et al. (2011b) demonstrated that dynamio action in accretion only occurs for resolutions of at least 30 cells per Jeans length, and does not show convergence out to at least 128 cells per Jeans length, instead showing continuously stronger growth of rms field with higher resolution and higher effective Reynolds number (Federrath et al. 2011a). Balsara et al. (2004) had already shown that supernova-driven turbulence in a periodic box acts as a turbulent dynamio. Hill et al. (2011) shows that this likely holds in a stratified medium as well, with magnetic field energies initially varying dependent on their initial values but then appearing to converge towards values characteristic of field strengths somewhat under $5 \mu\text{G}$. However runs of 400 Myr still had not clearly moved into a steady-state regime, so this conclusion remains preliminary.

4. Conclusions

Supernova-driven turbulence appears increasingly likely to be able to explain observations in $H\alpha$ and X-ray of material above the plane of the Galaxy, along with many other observations. Hypersonic vertical motions of large regions of galactic halos above star-forming disks appear to be driven by transient variations in energy input in the much denser disk midplanes of the galaxies, as predicted by Walters & Cox (2001). These vertical motions appear to explain at least some of the discrepancies between models and observations identified by Henley et al. (2010) and Wood et al. (2010). Our magnetized models demonstrated that magnetic fields can be modeled stably even in highly compressible, highly magnetized flows using the positivity preserving HLL3R solver described by Waagan (2009). They further suggested that a turbulent dynamo can be driven in a stratified disk, as well as in a periodic box.

Acknowledgments. This work was partly supported by NASA/SAO grant TM0-11008X and by NSF grant AST-0607512. The software used in this work was in part developed by the DOE NNSA-ASC OASCR Flash Center at the University of Chicago.

References

- Avillez, M. A. 2000, *MNRAS*, 315, 479
 Balsara, D. S., Kim, J., Mac Low, M.-M., & Mathews, G. J. 2004, *ApJ*, 617, 339
 Bouchut, F., Klingenberg, C., & Waagan, K. 2007, *Numer. Math.*, 108, 7
 — 2010, *Numer. Math.*, 115, 647
 Brunt, C. M., Federrath, C., & Price, D. J. 2010, *MNRAS*, 403, 1507
 Federrath, C., Chabrier, G., Schober, J., Banerjee, R., Klessen, R. S., & Schleicher, D. R. G. 2011a, *Physical Review Letters*, 107, 114504
 Federrath, C., Sur, S., Schleicher, D. R. G., Banerjee, R., & Klessen, R. S. 2011b, *ApJ*, 731, 62
 Fryxell, B., Olson, K., Ricker, P., Timmes, F. X., Zingale, M., Lamb, D. Q., MacNeice, P., Rosner, R., Truran, J. W., & Tufo, H. 2000, *ApJS*, 131, 273
 Haffner, L. M., Reynolds, R. J., Tufo, S. L., Madsen, G. J., Jaehnig, K. P., & Percival, J. W. 2003, *ApJS*, 149, 405
 Harten, A., Lax, P. D., & van Leer, B. 1983, *SIAM Rev.*, 25, 35
 Henley, D. B., Shelton, R. L., Kwak, K., Joung, M. R., & Mac Low, M.-M. 2010, *ApJ*, 723, 935
 Hill, A. S., Benjamin, R. A., Kowal, G., Reynolds, R. J., Haffner, L. M., & Lazarian, A. 2008, *ApJ*, 686, 363
 Hill, A. S., Joung, M. R., Mac Low, M.-M., Benjamin, R. A., Haffner, L. M., Klingenberg, C., & Waagan, K. 2011, *ApJ*, submitted
 Joung, M. K. R., & Mac Low, M.-M. 2006, *ApJ*, 653, 1266
 Joung, M. R., Mac Low, M.-M., & Bryan, G. L. 2009, *ApJ*, 704, 137
 Mac Low, M.-M., & Klessen, R. S. 2004, *Reviews of Modern Physics*, 76, 125
 Sur, S., Schleicher, D. R. G., Banerjee, R., Federrath, C., & Klessen, R. S. 2010, *ApJ*, 721, L134
 Tamburro, D., Rix, H.-W., Leroy, A. K., Mac Low, M.-M., Walter, F., Kennicutt, R. C., Brinks, E., & de Blok, W. J. G. 2009, *AJ*, 137, 4424
 Waagan, K. 2009, *Journal of Computational Physics*, 228, 8609
 Waagan, K., Federrath, C., & Klingenberg, C. 2011, *Journal of Computational Physics*, 230, 3331
 Walters, M. A., & Cox, D. P. 2001, *ApJ*, 549, 353
 Wood, K., Hill, A. S., Joung, M. R., Mac Low, M.-M., Benjamin, R. A., Haffner, L. M., Reynolds, R. J., & Madsen, G. J. 2010, *ApJ*, 721, 1397